

# Mid-infrared carbon monoxide detection system using differential absorption spectroscopy technique\*

DONG Ming (董明)<sup>1</sup>, SUI Yue (隋越)<sup>1</sup>, LI Guo-lin (李国林)<sup>1</sup>, ZHENG Chuan-tao (郑传涛)<sup>1\*\*</sup>, CHEN Mei-mei (陈玫玫)<sup>2\*\*</sup>, and WANG Yi-ding (王一丁)<sup>1</sup>

1. State Key Laboratory on Integrated Optoelectronics, College of Electronic Science and Engineering, Jilin University, Changchun 130012, China

2. College of Communication Engineering, Jilin University, Changchun 130012, China

(Received 3 August 2015)

©Tianjin University of Technology and Springer-Verlag Berlin Heidelberg 2015

A differential carbon monoxide (CO) concentration sensing device using a self-fabricated spherical mirror (e.g. light-collector) and a multi-pass gas-chamber is presented in this paper. Single-source dual-channel detection method is adopted to suppress the interferences from light source, optical path and environmental changes. Detection principle of the device is described, and both the optical part and the electrical part are developed. Experiments are carried out to evaluate the sensing performance on CO concentration. The results indicate that at  $1.013 \times 10^5$  Pa and 298 K, the limit of detection (LoD) is about  $11.5 \text{ mg/m}^3$  with an absorption length of 40 cm. As the gas concentration gets larger than  $115 \text{ mg/m}^3$  ( $1.013 \times 10^5$  Pa, 298 K), the relative detection error falls into the range of  $-1.7\%$ — $+1.9\%$ . Based on 12 h long-term measurement on the  $115 \text{ mg/m}^3$  and  $1150 \text{ mg/m}^3$  CO samples, the maximum detection errors are about 0.9% and 5.5%, respectively. Due to the low cost and competitive characteristics, the proposed device shows potential applications in CO detection in the circumstances of coal-mine production and environmental protection.

**Document code:** A **Article ID:** 1673-1905(2015)06-0469-4

**DOI** 10.1007/s11801-015-5151-6

Monitoring toxic and flammable gases, such as methane ( $\text{CH}_4$ ), carbon monoxide (CO), sulfur dioxide ( $\text{SO}_2$ ), shows wide applications in the fields of environmental protection, industrial processing control, medical diagnosis, and chemical analysis<sup>[1-5]</sup>. Infrared CO sensing device<sup>[6-11]</sup> has the advantages of wide measuring range, fast response, high sensitivity, and good selectivity. Therefore, infrared absorption spectroscopy becomes the most popular detection technique. The existing infrared sensing techniques can be classified into three types, namely, photoacoustic spectroscopy (PAS)<sup>[6]</sup>, wavelength modulation spectroscopy (WMS) or tunable diode laser absorption spectroscopy (TDLAS)<sup>[7-10]</sup>, and direct absorption spectroscopy (DAS)<sup>[11]</sup>. PAS-based detection system has high sensitivity, but it is not suitable for in-situ detection<sup>[6]</sup>. Although TDLAS-based system has good detection performance, the diode lasers require cryogenic cooling and generally should be operated in a multi-mode manner<sup>[10]</sup>. Besides, because of expensive infrared lasers and complicated optical gas-cell structure, it is difficult to put this kind of sensing devices into wide application. Therefore, the laser-based gas detection systems are undesirable especially in the cases which only

require portable, simple, and low-cost sensing device. Consequently, a compromise selection between cost and performance is considered in this paper. Based on DSA technique, we present a differential mid-infrared CO detection system using a low-cost wideband mid-infrared light source and a dual-channel pyroelectric detector with the detection channel at  $4.643 \mu\text{m}$  and the reference channel at  $3.947 \mu\text{m}$ .

The structure of our CO detection device is shown in Fig.1. A field programmable gate array (FPGA) processor is used as the primary control and processing component. A spherical mirror is used as absorption pool as well as light-collector. A wide-band mid-infrared light source (IR55) and a dual-channel mid-infrared detector equipped with two optical filters are located at the upper side and lower side, respectively. The 4 Hz square-wave modulation signal with a constant current at ON-state is supplied to the infrared light source. There are two channels during detection, namely, the detection channel and the reference channel. For the detection channel, the light reaching the  $4.643 \mu\text{m}$  filter will be absorbed by CO molecule and a detection signal will be generated. For the reference channel, the light reaching the  $3.947 \mu\text{m}$  filter

\* This work has been supported in part by the National Key Technology R&D Program of China (Nos.2013BAK06B04 and 2014BAD08B03), the National Natural Science Foundation of China (Nos.61307124 and 11404129), the Science and Technology Department of Jilin Province of China (Nos.20120707 and 20140307014SF), the Changchun Municipal Science and Technology Bureau (Nos.11GH01 and 14KG022), and the State Key Laboratory of Integrated Optoelectronics, Jilin University (No.IOSKL2012ZZ12).

\*\* E-mails: zhengchuantao@jlu.edu.cn; chenmm@jlu.edu.cn

will not be absorbed by CO molecule and a reference signal will be generated. These two electric signals are both processed by pre-amplifier (PA), band-pass filter (BPF), differential amplifier (DA), lock-in amplifier, sampling/holding (S/H), and finally converted to digital signals by the 16-bit analog-to-digital converter (ADC).

The infrared light source IR55 is a wideband infrared source. The source is fabricated with micro-electromechanical system (MEMS) technology, which has the advantages of wide spectral range, fast response, high modulation depth, high efficiency, low power consumption, and long life. Owing to the slow response of the pyroelectric detector, we choose 4 Hz as its modulation frequency. The used detector is a PerkinElmer's dual-channel pyroelectric detector, whose specific detectivity ( $D^*$ ) is  $3.5 \times 10^8 \text{ cm} \cdot \text{Hz}^{1/2} / \text{W}$ . Pyroelectric detector is made based on the principle of pyroelectricity, which is the ability of certain materials to generate a temporary voltage when they are heated or cooled. The change in temperature modifies the positions of the atoms slightly within the crystal structure, and thus changes the polarization of the material. This polarization change generates a voltage across the crystal.

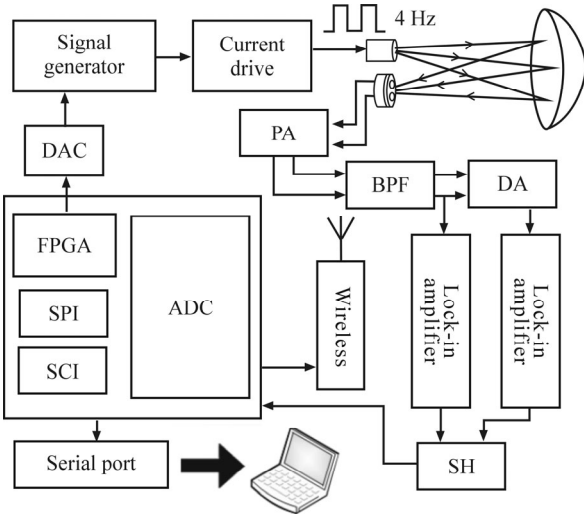


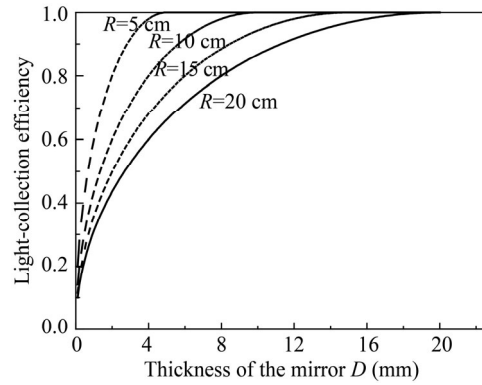
**Fig.1 Schematic diagram of the mid-infrared CO detection device**

Define the divergence angle of the light source as  $\theta$ . For the spherical mirror, define its radius as  $R$ , height as  $H$ , and thickness as  $D$ , as marked in Fig.2(b). The light-collection efficiency (defined as  $\eta$ ) is obtained by

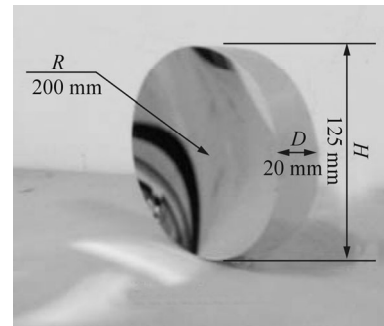
$$\eta = \begin{cases} \frac{\sqrt{R^2 - (R-D)^2}}{R \sin \theta} & D < R(1 - \cos \theta) \\ 1 & D \geq R(1 - \cos \theta) \end{cases} \quad (1)$$

Using Eq.(1), the curves of  $\eta$  versus the parameters of the spherical reflector are plotted in Fig.2(a). In order to get a high light collection efficiency and a doubled absorption length, the parameter values of the aluminized spherical reflector are taken as  $R=200 \text{ mm}$ ,  $D=20 \text{ mm}$ , and  $H=125 \text{ mm}$ . The photograph of the aluminized

spherical reflector is shown in Fig.2(b).



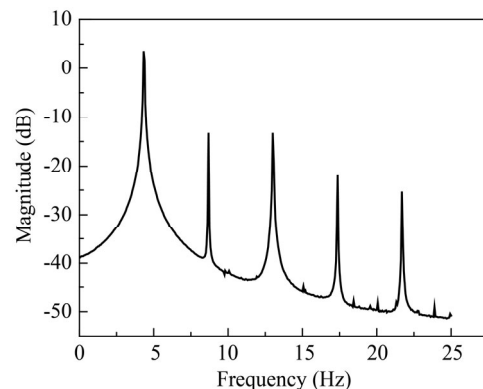
(a)



(b)

**Fig.2 (a) Curves of the light-collection efficiency  $\eta$  versus the thickness of the mirror  $D$ ; (b) The photograph of the aluminized spherical reflector mirror**

When the light source is not modulated (namely, the light source is set as OFF state), the output signals from the detector are exactly the system noises, and they mainly contain 50 Hz noise and white noise. Their levels will influence the detection sensitivity of CO concentration. When the light source is modulated, the two analog signals output from the dual-channel detector are both processed by PA and BPF. In this case, the measured spectra of them are shown in Fig.3. It can be found that at 4 Hz frequency, the 10 dB bandwidth is less than 1 Hz, which suggests high signal-to-noise ratio (SNR) of the system.



(a) Detection channel

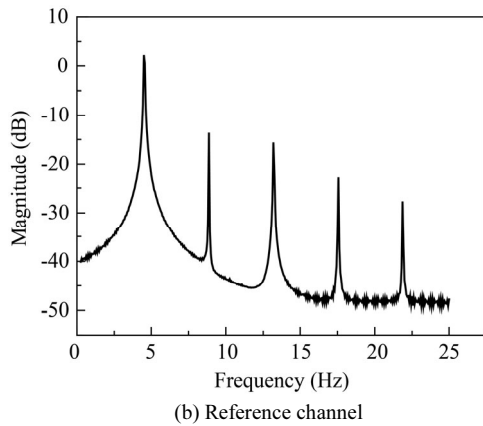


**Fig.3** With the infrared source at modulation state, the measured spectra of the two output signals from (a) detection channel and (b) reference channel

During experiment, we put our developed device into the plastic box. The gas sample is prepared in the box, and the gas can diffuse into the gas-cell through its side shutters. The concentrations of the prepared standard CO samples within the concentration range of 0—1 380 mg/m<sup>3</sup> (1.013×10<sup>5</sup> Pa, 298 K, similar as below) are measured using the developed sensing device. The experimental results of the relation between  $\delta U(\lambda_1, \lambda_2, l) / U(\lambda_2, l)$  and  $C$  (mg/m<sup>3</sup>) are shown in Fig.4. The exponential function of the fitting curve is obtained as

$$\delta U(\lambda_1, \lambda_2, l) / U(\lambda_2, l) = -0.017 13 \times \exp(-0.002 7 \times C) + 0.113 95. \quad (2)$$

The limit of detection (LoD) is the minimum increase of the concentration from 0 mg/m<sup>3</sup> that can produce a variation in the denoised peak-to-peak voltage-ratio clearly recognized by the ADC. Then proper amount of pure CO is repeatedly injected into the container until the measured differential-ratio is steadily higher than the ratio at 0 mg/m<sup>3</sup>. Then the total volume of the injected CO is the LoD. From the inset in Fig.4, the measured differential-ratio is not obviously different from the ratio at 0 mg/m<sup>3</sup> until the gas concentration gets larger than 11.5 mg/m<sup>3</sup>. So we can determine that the LoD of the system is about 11.5 mg/m<sup>3</sup>.

To measure the detection accuracy, 18 standard gas samples are prepared. Let the gas pass through the gas-cell, and their concentrations are determined by the measured ratio of  $\delta U(\lambda_1, \lambda_2, l) / U(\lambda_2, l)$ . The relative errors of all gas samples are calculated, and the results are shown in Fig.5(b). When the CO concentration is as low as 11.5 mg/m<sup>3</sup>, the error reaches the maximum value up to +6.5%. As the concentration gets larger than 115 mg/m<sup>3</sup>, the error falls into the range of -1.7%—+1.9%. From this point of view, the developed device reveals acceptable performance.

Because of noises and interferences introduced in the differential-ratio signal, the detection stability may be affected. For the two prepared gas samples with the con-

centrations of 115 mg/m<sup>3</sup> and 1 150 mg/m<sup>3</sup>, 12 h detection is carried out, and the results are averaged per half an hour. For the 115 mg/m<sup>3</sup> gas sample, the measured concentration range is 114.8—116.0 mg/m<sup>3</sup>, indicating an absolute error less than 0.9%, as shown in Fig.6(a). For the 1 150 mg/m<sup>3</sup> gas sample, the measured concentration range is 1 145.4—1 213.3 mg/m<sup>3</sup>, indicating an absolute error less than 5.5%, as shown in Fig.6(b). The errors obtained from the stability curve also coincide with those shown in Fig.5.

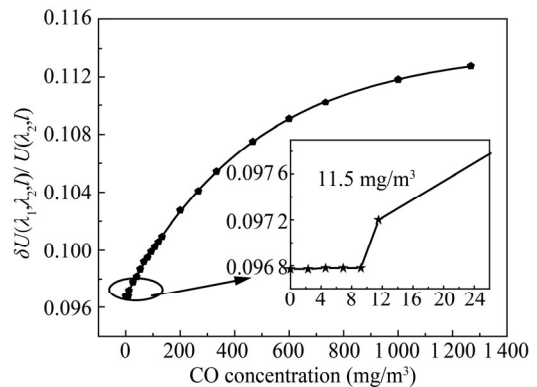


**Fig.4** Experimental data and fitting curve of the measured differential-ratio  $\delta U(\lambda_1, \lambda_2, l) / U(\lambda_2, l)$  versus the CO concentration  $C$

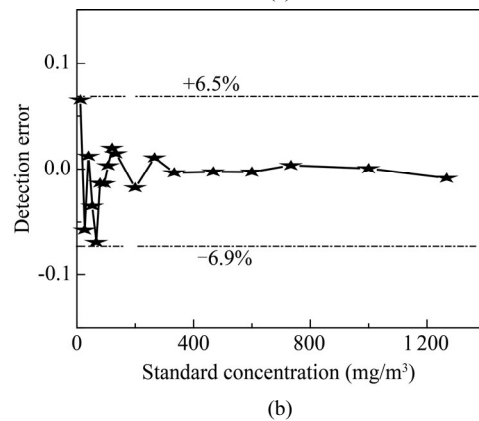
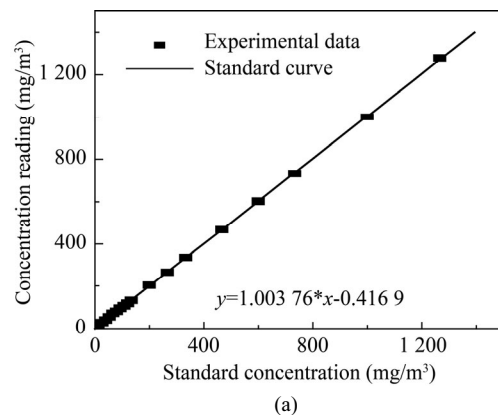


**Fig.5** By using the developed sensing device, (a) the measured concentration and (b) the relative error on the standard gas samples whose concentration range is 0—1 380 mg/m<sup>3</sup>

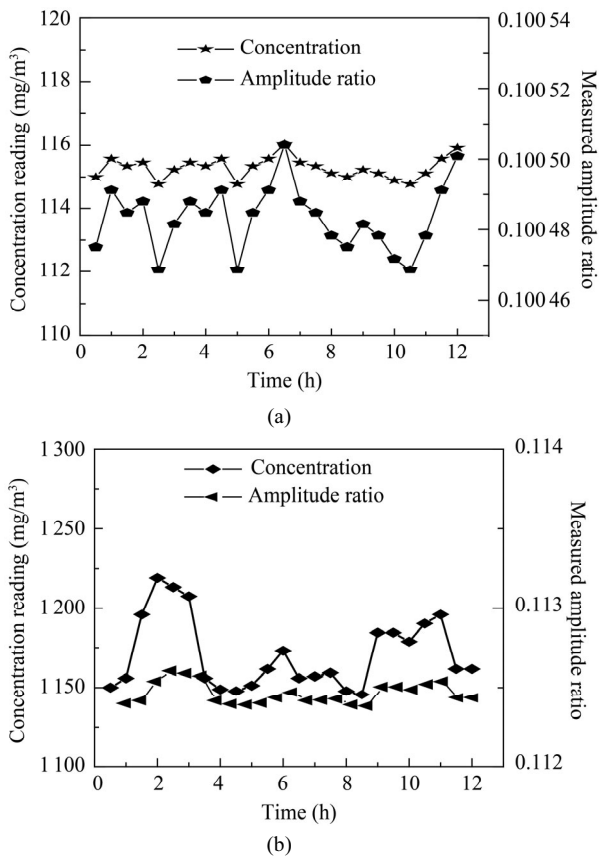


**Fig.6 The long-term measurement results of the concentration and the differential-ratio on the two CO samples with the concentrations of (a) 115 mg/m<sup>3</sup> and (b) 150 mg/m<sup>3</sup>**

As exhibited in Tab.1, the performance of our portable device is compared with those of other reported CO detection devices or sensors<sup>[12,13]</sup>. Though the absorption length in Ref.[12] reaches 256 cm, the measured limit of detection (LoD) is only 7.475 mg/m<sup>3</sup>. This is because the absorption line strength at 2.3 μm is two orders of magnitude lower than that at 4.6 μm. In Ref.[13], a quantum cascaded laser (QCL) at 4.6 μm is adopted, which can utilize the strongest absorption of CO molecule. So with an absorption length of 100 cm, the LoD is as low as

**Tab.1 Comparison of the performance between this device and other reported CO detection devices**

Scheme	Source/ Wavelength (μm)	Absorption length (cm)	LoD (mg/m <sup>3</sup> )	Measurement temperature (°C)	Cost
Ref.[12]	Near-IR DFBL/2.3	256	7.475	900	High
Ref.[13]	Mid-IR QCL/4.62	100	0.035	25	High
This paper	Incandescence/4.66	40	11.5	25	Low

0.035 mg/m<sup>3</sup>. With an absorption length of only 40 cm, the LoD of the proposed device is at the same level with that in Ref.[12]. Furthermore, the used incandescence light source is extremely cheap compared with the laser sources in Refs.[12] and [13].

In summary, a differential mid-infrared CO concentration detection device is experimentally demonstrated by employing a spherical-mirror-based multi-pass chamber to suppress the interferences resulting from the light source, the optical path and the environmental changes. The detection principle is described, and key modules including the optical part and the electrical part are designed and fabricated. Experiments are carried out to evaluate the detection performance. At 1.013×10<sup>5</sup> Pa and 298 K, the LoD is about 11.5 mg/m<sup>3</sup>, and the relative detection error falls into the range of -1.7%—+1.9% as the concentration gets larger than 115 mg/m<sup>3</sup>. Based on 12 h long-term measurement on the 115 mg/m<sup>3</sup> and 150 mg/m<sup>3</sup> CO samples, the maximum detection errors are about 0.9% and 5.5%, respectively. The proposed device shows potential applications in CO detection in coal-mine production and environmental protection.

## References

- [1] J. Li, U. Parchatka and H. Fischer, *Anal. Methods* **6**, 5483 (2014).
- [2] L. Tao, K. Sun, D. J. Miller, D. Pan, L. M. Golston and M. A. Zondlo, *Appl. Phys. B* **119**, 153 (2015).
- [3] R. M. Spearrin, C. S. Goldenstein, I. A. Schultz, J. B. Jeffries and R. K. Hanson, *Appl. Phys. B* **117**, 689 (2014).
- [4] K. Sun, L. Tao, D. J. Miller, M. A. Khan and M. A. Zondlo, *Environ. Sci. Technol.* **48**, 3943 (2014).
- [5] J. Li, U. Parchatka and H. Fischer, *Sens. Actuators B: Chem.* **182**, 659 (2013).
- [6] T. Chen, G.F. Su and H.Y. Yuan, *Sens. Actuators B: Chem.* **109**, 233 (2005).
- [7] R. M. Spearrin, C. S. Goldenstein, J. B. Jeffries and R. K. Hanson, *Appl. Opt.* **53**, 1938 (2014).
- [8] R. Engelbrecht, *Spectrochimica Acta Part A.* **60**, 3291 (2004).
- [9] J. Vanderover, W. Wang and M.A. Oehlschlaeger, *Appl. Phys. B.* **103**, 959 (2011).
- [10] C.L. Schiller, H. Bozem, C. Gurk, U. Parchatka, R. Konigstedt, G.W. Harris, J. Lelieveld and H. Fischer, *Appl. Phys. B.* **92**, 419 (2008).
- [11] J. Vanderover and M.A. Oehlschlaeger, *Appl. Phys. B.* **99**, 353 (2010).
- [12] V. Ebert, H. Teichert, P. Strauch, T. Kolb, H. Seifert and J. Wolfrum, *Proc. Combust. Inst.* **30**, 1611 (2005).
- [13] J. Vanderover, W. Wang and M.A. Oehlschlaeger, *Appl. Phys. B* **103**, 959 (2011).